Hindawi Publishing Corporation
Journal of Nanomaterials
Volume 2012, Article ID 259684, 6 pages
doi:10.1155/2012/259684

Research Article

Cycling Performance of Nanocrystalline $LiMn_2O_4$ Thin Films via Electrophoresis

S. Parvathy, R. Ranjusha, K. Sujith, K. R. V. Subramanian, N. Sivakumar, Shantikumar V. Nair, and Avinash Balakrishnan

Nanosolar Division, Amrita Center for Nanosciences, Kochi 682 041, India

Correspondence should be addressed to
Shantikumar V. Nair, shantinair@aims.amrita.edu and Avinash Balakrishnan, avinash.balakrishnan@gmail.com

Received 9 January 2012; Revised 20 March 2012; Accepted 21 March 2012

Academic Editor: Ali Eftekhari

The present study demonstrates a novel approach by which titanium foils coated with $LiMn_2O_4$ nanocrystals can be processed into a high-surface-area electrode for rechargeable batteries. A detailed study has been performed to elucidate how surface morphology and redox reaction behaviors underlying these electrodes impact the cyclic and capacity behavior. These nanocrystals were synthesized by in situ sintering and exhibited a uniform size of ~55 nm. A direct deposition technique based on electrophoresis is employed to coat $LiMn_2O_4$ nanocrystals onto titanium substrates. From the analysis of the relevant electrochemical parameters, an intrinsic correlation between the cyclability and particle size has been deduced and explained in accordance with the Li intercalation/deintercalation process. Depending on the particle size incorporated on these electrodes, it is seen that in terms of capacitance fading, for nanoparticles cyclability is better than their micron-sized counterparts. It has been shown that electrodes based on such nanocrystalline thin film system can allow significant room for improvement in the cyclic performance at the electrode/electrolyte interface.

1. Introduction

Cubic spinel $LiMn_2O_4$ has been widely researched for its performance in secondary storage devices [1–4]. $LiMn_2O_4$ spinel structure consists of a cubic close-packed array of O^{2-}, Mn^{3+}, and possible Mn^{4+} that are located in the octahedral sites and Li^+ in the tetrahedral site. The Mn^{3+} has an octahedral coordination to the oxygens, which forms three-dimensional MnO_6 octahedra that act as host for Li^+. The combination of these structural features makes spinel $LiMn_2O_4$ a stable compound in different electrolytes for storage applications. In a Lithium ion battery, during the electrochemical reactions, Li^+ intercalates through the electrolyte, which involves three reaction stages, (i) Li^+ diffusion within the electrode, (ii) Li^+ transfer (charge transfer reaction) at the interface between the electrode and electrolyte, and (iii) finally the movement of Li^+ in the electrolyte. The first stage is the rate-determining step, which governs the performance of the batteries that depends on both the phase and surface morphology of the electrode material. This means that by maintaining phase purity and effectively increasing their surface area through nano-structuring it is possible to enhance the kinetic properties of the electrode system by decreasing the diffusion length [5]. For fabricating high-performance $LiMn_2O_4$ electrodes, many high-temperature techniques have been reported, for example, pulsed laser deposition [6, 7], spray pyrolysis [8, 9], combustion method [10, 11], and so forth; however, not much has been reported on the electrophoretic deposition of $LiMn_2O_4$. One of the main reasons has been the requirement of high voltage in volatile electrolytes, and also it is difficult to deposit micron-sized particles due to their inherent size and mass. For instance, studies have shown [12] that at a high voltage of 400 V, submicronic $LiMn_2O_4$ can be electrophoretically deposited. However, at this high voltage especially with the acetone type electrolyte, the reaction can be hazardous and extremely volatile. The present study reports the first examples of direct deposition of $LiMn_2O_4$ nanocrystals as thin films

onto Ti foils using a novel low-voltage (60 V) electrophoretic deposition technique. These electrodes exhibited a capacity of 147 mAh/g and capacity fade of 5% after 25 cycles.

2. Material and Methods

10 g of citric acid ($C_6H_7O_8$ NICE chemicals, India) was completely dissolved in 10 mL of double distilled water. To this solution, 0.75 g of lithium carbonate (Li_2CO_3 NICE chemicals, India) and 9.8 g of manganese acetate ($Mn(CH_3COO)_2$ NICE chemicals, India) were added and completely dissolved by rigorously stirring for 30 min at room temperature. 0.2 mL of ethylene glycol ($C_2H_8O_2$ NICE chemicals, India) was added to this solution. The pH of the solution was measured as 4. The pH of this solution was increased to 10 by dropwise addition of ammonia, resulting into a viscous brown-colored solution. This solution was kept for calcination by heating it at 140°C for 3 hr in air, after which the temperature was increased at a ramp rate of 5 C/min to 800°C for 3 hr. Furnace cooling was employed, after the calcination. The particle size and morphology of the resultant powder were analyzed using transmission electron microscopy (TEM,) and X-ray diffractometry (XRD, X'Pert PRO Analytical). The oxidation states of the synthesized powder were analyzed using X-ray photospectroscopy (XPS, Axis Ultra, Shimadzu).

The resultant $LiMn_2O_4$ nanopowders were used for electrophoretic deposition. For this an electrochemical setup was employed, comprising of titanium foil (1 cm × 1 cm × 0.2 mm) and platinum mesh used as an cathode and anode, respectively. Electrolyte consisted of solution of pure isopropanol (20 mL). To this electrolyte, 12 mg of $LiMn_2O_4$ powders was dispersed uniformly under constant stirring. The deposition was carried out at 60 V for 3 hr at room temperature resulting in a thin uniform layer of $LiMn_2O_4$. Scanning electron microscopy (SEM, Model: JEOL JSM 6490 LA) was performed to analyze the surface of the electrodeposited $LiMn_2O_4$ layer. The particle size distribution was measured using Image J software from the TEM images. For electrophoretically deposited $LiMn_2O_4$, the thickness of the coating was measured using a surface profilometer (Veeco Dektak 150). Cyclic voltammetry (CV, electrochemical workstation: Newport Model) studies were done to evaluate the electrochemical performance of the electrophoretically deposited $LiMn_2O_4$ layer, which was kept as the working electrode in a three-electrode setup configuration. The reference and counterelectrode consisted of calomel and platinum. The electrolyte used for this purpose was 1 M lithium perchlorate in propylene carbonate.

3. Results and Discussion

Figure 1 shows the XRD pattern of the synthesized $LiMn_2O_4$ nanocrystals. Its diffraction peaks were perfectly indexed to a pure cubic spinel phase (JCPDS: 35–782). In addition, the broad diffraction peaks of the powder indicated that its particle size was small. Peak broadening in nanoparticles can originate from variations in lattice spacings, caused by lattice strain as the size decreases; the crystallite size was estimated as 40 ± 5 nm using the Scherrer equation [13].

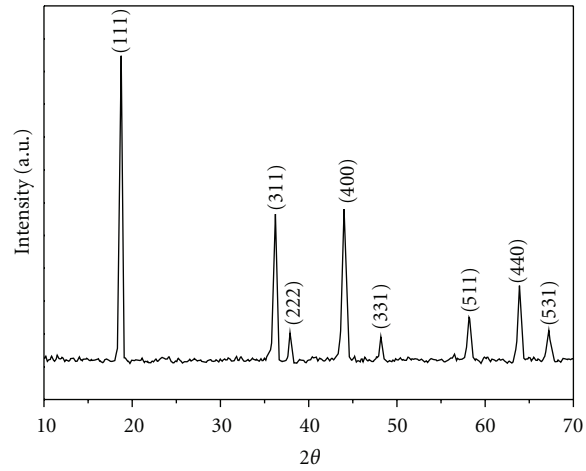

Figure 1: XRD of $LiMn_2O_4$ nanocrystals.

TEM images displaying the morphology of $LiMn_2O_4$ are shown in Figure 2(a). It was found from high-resolution TEM (Figure 2(b)) that the interplanar spacings were about 0.6 nm showing a crystal orientation along the (111). This was confirmed by fast fourier transform (FFT) analysis (Figure 2(c)). The particle size analysis (Figure 2(d)) showed a skewed bimodal narrow distribution and was found to be in the range of 40–100 nm and primarily centered at ~55 nm.

The elemental composition and the valence states of the synthesized nanocrystals were done using XPS. Figure 3 gives the wide spectrum of $LiMn_2O_4$ crytals from 1200 to 200 eV. The presence of Li was distinctly detected in the powders at 54.5 eV. The Mn 2p peaks were deconvoluated (Figure 3 (inset)) at high resolution to reveal Mn 2p doublet for $LiMn_2O_4$. Similar patterns have been reported in the literature elsewhere [4, 14]. The Mn 2p core-level spectra showed a typical two-peak structure ($2p_{3/2}$ and $2p_{1/2}$) due to the spin-orbit splitting. The XPS spectrum was calibrated to the C_{1s} line, which was located at 285 eV. Using this reference, the peaks at 642.5 and 654.3 eV are attributed to Mn $2p_{3/2}$ and Mn $2p_{1/2}$, respectively. Studies have shown [14, 15] that the Mn $2p_{3/2}$ gives the XPS binding energy of Mn^{3+} and Mn^{4+} ions at 641.9 and 643.2 eV (in the present study this is shown as convoluted peaks in Figure 3 inset), respectively, which were in proximity to the values that were obtained in this study indicating the presence of mixed valence state of Mn ions in the synthesized nanocrystals.

The possible formation of stoichiometrically stable spinel $LiMn_2O_4$ (*Fd3m* is the space group and lattice parameter a = 8.247Å) nanocrystals with the precursors used in the present study can be explained through the following reaction stages. Mn^{2+} undergoes hydrolysis resulting in $MnOH^+$ [4] with the release of proton into the solution. $MnOH^+$ are complexed by citric acid which chelates these ions at pH = 10. The possible esterification [16] occurs in the presence of ethylene glycol at 140°C, which results in gel formation. Further heating of this gel provides sites for the incorporation of

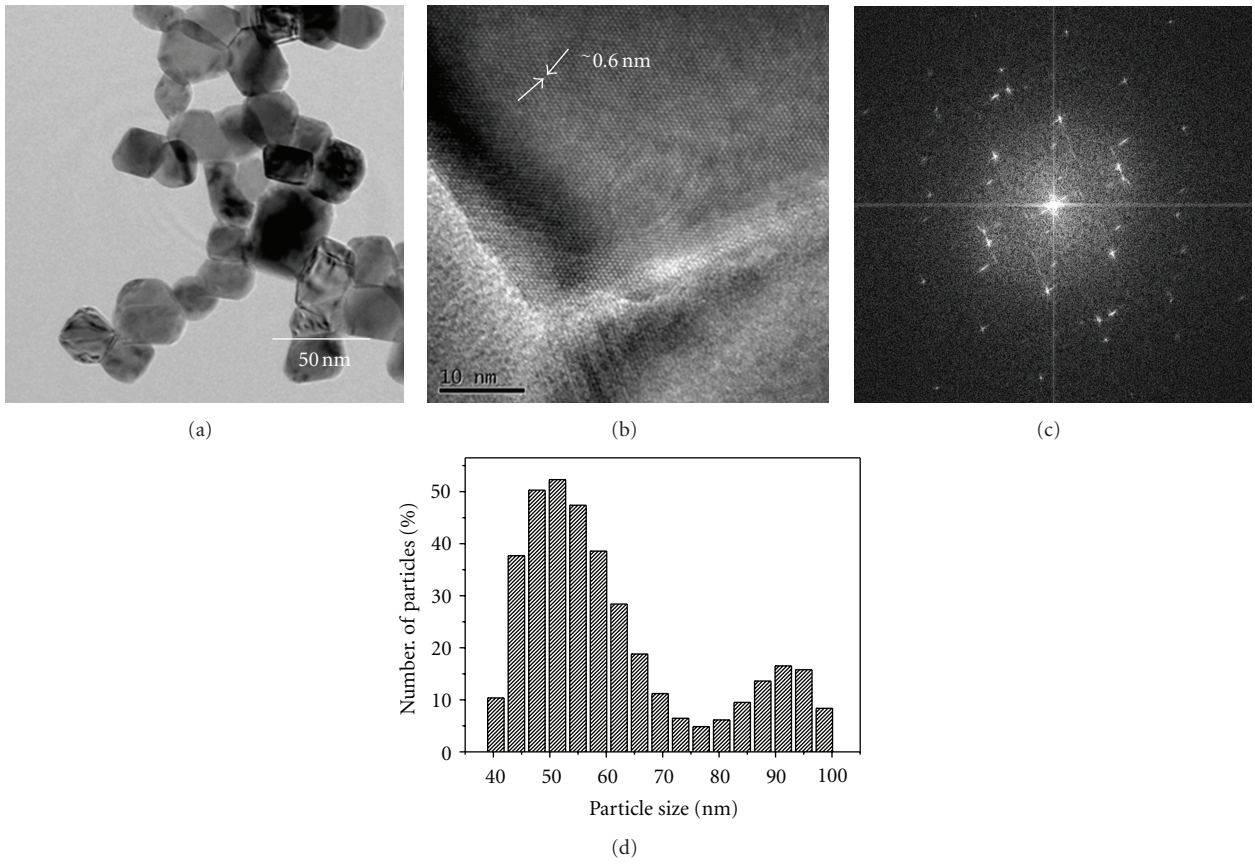

Figure 2: (a) TEM image; (b) HR-TEM image; (c) FFT patterns; (d) particle size distribution of $LiMn_2O_4$ nanocrystals.

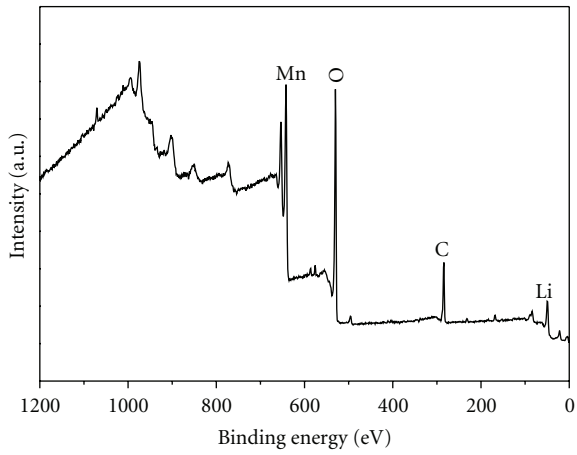

Figure 3: XPS of $LiMn_2O_4$ nanocrystals.

Li^+ into the Mn (II) complex to produce $LiMn_2O_4$ nanoparticles. The layout of possible chemical reactions for the above mechanism is shown in Figure 4. Figure 5(a) shows the surface morphology of the electrodeposited $LiMn_2O_4$ nanoparticle layer which exhibited a dense coating layer. Surface profilometry on this layer exhibited a highly roughened surface ($R_a = 800 \pm 90$ nm) and thickness of 5–8 μm (as shown in Figure 5(b)).

Figure 6(a) shows a typical cyclic voltammogram (scan rate: 1 mv/s) of the $LiMn_2O_4$ electrode. Four distinct peaks were identified on the CV pattern corresponding to different states of charge-discharge. These peaks were in accordance with the Li intercalation/deintercalation process and can be written as follows [17–21].

(i) Reaction from (A) to (B):

$$LiMn_2O_4(A) \longleftrightarrow Li_{0.5}Mn_2O_4(B) + 0.5Li^+ + 0.5e^-. \quad (1)$$

(ii) Reaction from (B) to (C):

$$Li_{0.5}Mn_2O_4(B) \longleftrightarrow Mn_2O_4(C) + 0.5Li^+ + 0.5e^-. \quad (2)$$

(iii) Reaction from (D) to (E):

$$Mn_2O_4\ (D) + 0.5Li^+ + 0.5e^- \longleftrightarrow Li_{0.5}Mn_2O_4\ (E). \quad (3)$$

(iv) Reaction from (E) to (F):

$$Li_{0.5}Mn_2O_4\ (E) + 0.5Li^+ + 0.5e^- \longleftrightarrow LiMn_2O_4\ (F). \quad (4)$$

From Figure 6(a) the total capacity was calculated as 147 mAh/g, which is comparable to conventional micron-sized and bulk $LiMn_2O_4$ systems in the literature [18–20].

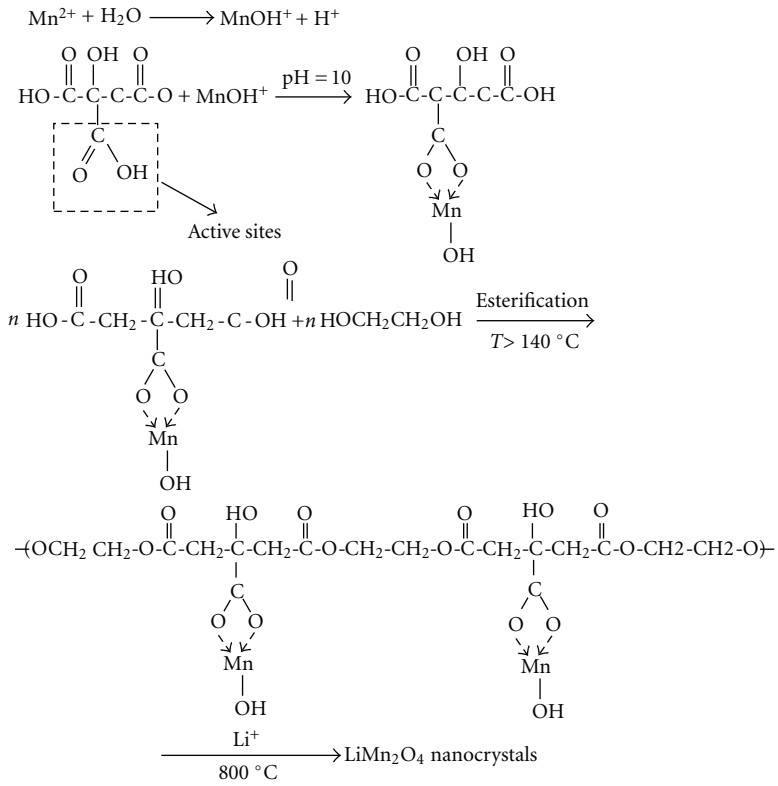

Figure 4: Schematic presentation of reaction mechanisms leading to the formation of $LiMn_2O_4$ nanocrystals.

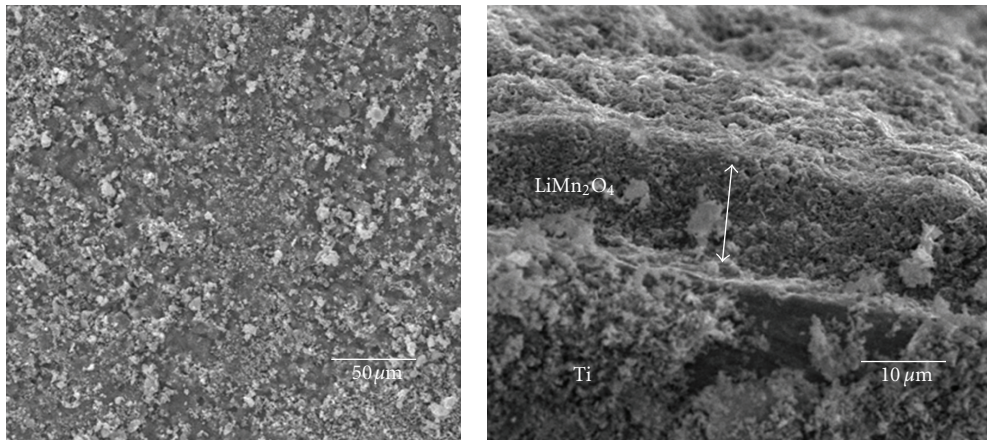

Figure 5: SEM image showing the electrophoretic deposition of $LiMn_2O_4$ nanocrystals over Ti substrate.

The cycling ability of $LiMn_2O_4$ electrode was evaluated by the capacity fade, which was obtained from CV curves (scan rate: 50 mv/s) as shown in Figure 6(b). The result in Figure 6(b) reveals that the capacity fade of the electrode at the end of 25th cycle was ~5%. It was observed that the cycling ability of the electrophoretically deposited $LiMn_2O_4$ layer was stable, which can be attributed to the release of more Mn^{4+} cations that limit the Jahn-Teller distortion effect [22] encountered in octahedral complexes of the transition metals like those of $LiMn_2O_4$.

Further, the structural stability of the coating layer can also play an important role in determining the capacity of the electrode overlay. The formation of a thin and porous layer of $LiMn_2O_4$ can readily accommodate the microscopic stresses due to the any-dimensional changes within an electrode, for example, stresses arising during the phase transformation of cubic to tetragonal phase in $LiMn_2O_4$ during charge-discharge cycle.

Figure 7 shows the charge-discharge profile of $LiMn_2O_4$ at a discharging current density of 5 mA/g using 1 M lithium

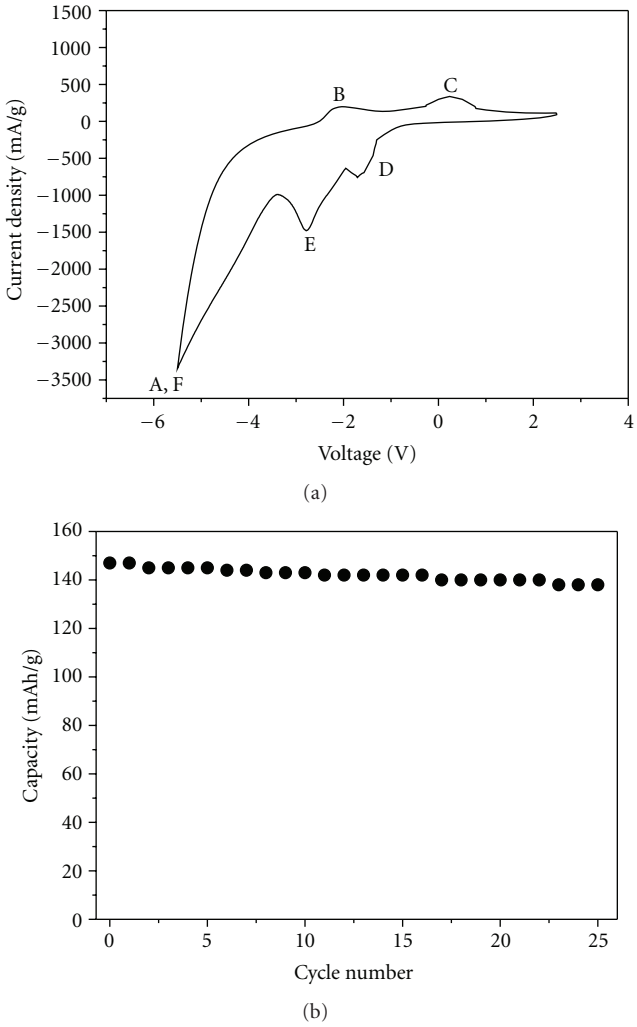

Figure 6: CV studies on electrophoretically deposited $LiMn_2O_4$ at (a) 1 mV/s and (b) capacity versus cycle number.

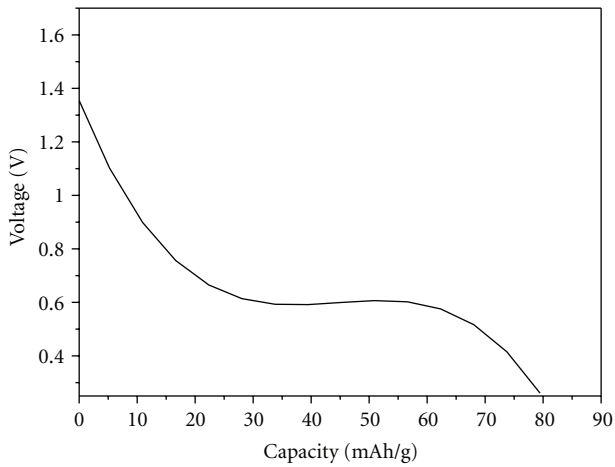

Figure 7: Voltage versus capacity curve from charge-discharge profile.

perchlorate in propylene carbonate. The capacity obtained from this curve was found to be ~80 mAh/g. It was found that when a micron-sized particulate structure of $LiMn_2O_4$ (~10 μm particle size) was deposited electrophoretically under similar conditions, the direct consequence was peeling and delamination of the coating layer during the charge-discharge cycles. Thus, for such an electrode system, the nanosize of $LiMn_2O_4$ structures was critical in determining the final performance of the electrode.

4. Conclusions

The phase-pure $LiMn_2O_4$ spinel nanocrystals of uniform size ~55 nm were synthesized at 800°C. XPS studies showed the presence of mixed valence state of Mn ions in the synthesized nanocrystals. The surface morphology of the electrodeposited $LiMn_2O_4$ nanoparticle layer exhibited a dense coating layer with a highly roughened surface (R_a = 800 ± 90 nm) and thickness of 8–10 μm. CV studies showed four distinct peaks corresponding to different states of charge-discharge attributed to the Li intercalation/de-intercalation. The cyclability studies showed these electrodes to be stable, where the capacity fade of these electrodes at the end of the 25th cycle was found to be 5%. Charge the discharge profile of $LiMn_2O_4$ showed the capacity to be ~80 mAh/g. The present study opens an avenue for possible fabrication of thin film secondary storage batteries where $LiMn_2O_4$ nanocrystals can be deposited over scalable areas in a controlled fashion.

Acknowledgment

The Ministry of New Renewable Energy, Government of India is gratefully acknowledged for their financial support.

References

[1] K. S. Lee, S. T. Myung, H. G. Jung, J. K. Lee, and Y. K. Sun, "Spinel lithium manganese oxide synthesized under a pressurized oxygen atmosphere," *Electrochimica Acta*, vol. 55, no. 28, pp. 8397–8401, 2010.

[2] N. Yu, C. Shao, Y. Liu, H. Guan, and X. Yang, "Nanofibers of $LiMn_2O_4$ by electrospinning," *Journal of Colloid and Interface Science*, vol. 285, no. 1, pp. 163–166, 2005.

[3] B. J. Hwang, R. Santhanam, and D. G. Liu, "Effect of various synthetic parameters on purity of $LiMn_2O_4$ spinel synthesized by a sol-gel method at low temperature," *Journal of Power Sources*, vol. 101, no. 1, pp. 86–89, 2001.

[4] X. Wang, X. Chen, L. Gao et al., "Citric acid-assisted sol-gel synthesis of nanocrystalline $LiMn_2O_4$ spinel as cathode material," *Journal of Crystal Growth*, vol. 256, no. 1-2, pp. 123–127, 2003.

[5] K. T. Lee and J. Cho, "Roles of nanosize in lithium reactive nanomaterials for lithium ion batteries," *Nano Today*, vol. 6, no. 1, pp. 28–41, 2011.

[6] N. Kuwata, R. Kumar, K. Toribami, T. Suzuki, T. Hattori, and J. Kawamura, "Thin film lithium ion batteries prepared only by pulsed laser deposition," *Solid State Ionics*, vol. 177, no. 26–32, pp. 2827–2832, 2006.

[7] S. B. Tang, M. O. Lai, L. Lu, and S. Tripathy, "Comparative study of $LiMn_2O_4$ thin film cathode grown at high, medium and low temperatures by pulsed laser deposition," *Journal of Solid State Chemistry*, vol. 179, no. 12, pp. 3831–3838, 2006.

[8] H. M. Wu, J. P. Tu, Y. F. Yuan, Y. Li, X. B. Zhao, and G. S. Cao, "Structural, morphological and electrochemical characteristics of spinel $LiMn_2O_4$ prepared by spray-drying method," *Scripta Materialia*, vol. 52, no. 6, pp. 513–517, 2005.

[9] J. P. Tu, H. M. Wu, Y. Z. Yang, and W. K. Zhang, "Spray-drying technology for the synthesis of nanosized $LiMn_2O_4$ cathode material," *Materials Letters*, vol. 61, no. 3, pp. 864–867, 2007.

[10] R. M. Rojas, J. M. Amarilla, L. Pascual, J. M. Rojo, D. Kovacheva, and K. Petrov, "Combustion synthesis of nanocrystalline $LiNi_YCo_{1-2}YMn_{1+Y}O_4$ spinels for 5 V cathode materials. Characterization and electrochemical properties," *Journal of Power Sources*, vol. 160, no. 1, pp. 529–535, 2006.

[11] C. Z. Lu and G. T. K. Fey, "Nanocrystalline and long cycling $LiMn_2O_4$ cathode material derived by a solution combustion method for lithium ion batteries," *Journal of Physics and Chemistry of Solids*, vol. 67, no. 4, pp. 756–761, 2006.

[12] K. Kanamura, A. Goto, J. I. Hamagami, and T. Umegaki, "Electrophoretic fabrication of positive electrodes for rechargeable lithium batteries," *Electrochemical and Solid-State Letters*, vol. 3, no. 6, pp. 259–262, 2000.

[13] B. D. Cullity and S. R. Stock, *Elements of X Ray Diffraction*, Prentice Hall, Upper Saddle River, NJ, USA, 3rd edition, 2001.

[14] W. D. Pan, C. Hong, D. Fei et al., "Comparative studies on structure and electronic properties between thermal lithiated $Li0_{.5}MnO_2$ and $LiMn_2O_4$," *Chemical Research in Chinese Universities*, vol. 26, no. 2, pp. 283–286, 2010.

[15] K. M. Shaju, G. V. Subba Rao, and B. V. R. Chowdari, "Spinel phases, $LiM_{1/6}Mn_{11/6O_4}$ (M=Co, CoAl, CoCr, CrAl), as cathodes for lithium-ion batteries," *Solid State Ionics*, vol. 148, no. 3-4, pp. 343–350, 2002.

[16] M. Michalska, L. Lipińska, M. Mirkowska, M. Aksienionek, R. Diduszko, and M. Wasiucionek, "Nanocrystalline lithium-manganese oxide spinels for Li-ion batteries- Sol-gel synthesis and characterization of their structure and selected physical properties," *Solid State Ionics*, vol. 188, no. 1, pp. 160–164, 2011.

[17] A. Eftekhari, "On the fractal study of $LiMn_2O_4$ electrode surface," *Electrochimica Acta*, vol. 48, no. 19, pp. 2831–2839, 2003.

[18] W. S. Yoon, K. Y. Chung, K. H. Oh, and K. B. Kim, "Changes in electronic structure of the electrochemically Li-ion deintercalated $LiMn_2O_4$ system investigated by soft X-ray absorption spectroscopy," *Journal of Power Sources*, vol. 119-121, pp. 706–709, 2003.

[19] I. Yamada, T. Abe, Y. Iriyama, and Z. Ogumi, "Lithium-ion transfer at $LiMn_2O_4$ thin film electrode prepared by pulsed laser deposition," *Electrochemistry Communications*, vol. 5, no. 6, pp. 502–505, 2003.

[20] L. Feng, Y. Chang, L. Wu, and T. Lu, "Electrochemical behaviour of spinel $LiMn_2O_4$ as positive electrode in rechargeable lithium cells," *Journal of Power Sources*, vol. 63, no. 1, pp. 149–152, 1996.

[21] C. Y. Ouyang, S. Q. Shi, and M. S. Lei, "Jahn-Teller distortion and electronic structure of $LiMn_2O_4$," *Journal of Alloys and Compounds*, vol. 474, no. 1-2, pp. 370–374, 2009.

[22] T. F. Yi, C. L. Hao, C. B. Yue, R. S. Zhu, and J. Shu, "A literature review and test: structure and physicochemical properties of spinel $LiMn_2O_4$ synthesized by different temperatures for lithium ion battery," *Synthetic Metals*, vol. 159, no. 13, pp. 1255–1260, 2009.